

Cite this: *Soft Matter*, 2012, **8**, 2274

www.rsc.org/softmatter

PAPER

Effect of central linkages on mesophase behavior of imidazolium-based rod-like ionic liquid crystals†

Xiaohong Cheng,^{*a} Fawu Su,^a Rong Huang,^a Hongfei Gao,^a Marko Prehm^b and Carsten Tschierske^{*b}

Received 29th September 2011, Accepted 28th November 2011

DOI: 10.1039/c2sm06854k

Two series of phenylbenzylether and benzanilide based rod-like imidazolium bromides and their nonionic precursors, the 1-phenyl-1*H*-imidazoles have been synthesized and the influence of the number and length of the alkyl chain(s) and the structure of the linking group in the aromatic core (–CH₂O–, –COO–, –CONH–) on their mesophase self-assembly in ionic liquid crystalline phases were studied by POM, DSC and XRD. Upon decreasing the length of the *N*-terminal chain or by enlarging the number and length of the *C*-terminal chains, the sequence smectic (SmA)–hexagonal columnar (Col_{hex})–micellar cubic (Cub₁/*Pm3n*) was found for the ether based imidazolium salts; while only SmA and Col_{hex} phases were observed for the related amides. The influence of the polarity of the central linkages, namely –CH₂O– and –CONH–, on the mesophase structure and stability is discussed and compared with related –COO– connected ILC.

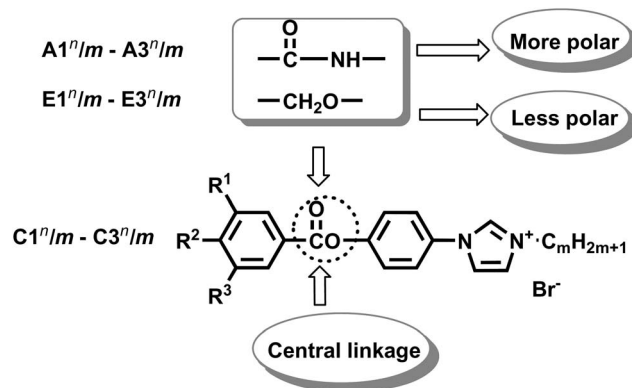
1. Introduction

Ionic self-assembly of soft matter provides interesting possibilities for producing well defined nanometre sized structures.¹ Such soft ionic materials can be used as adaptive ion conducting materials for batteries, fuel cells and capacitors.^{2–4} Also in living systems self-assembly of ionic soft matter is of significant importance, for example, in DNA self assembly,⁵ for the interactions of DNA with peptides⁶ and with anionic surfactants for gene delivery.^{7,8} Imidazolium based ionic liquid crystals (ILCs)^{9,10} combine the self-organization forces of liquid crystals with the unique solvent properties and ion-conducting properties of imidazolium based ionic liquids.¹¹ These LC materials lead to new applications, as for example in direction dependent ion-conducting materials,¹² and have improved the light-to-electric energy conversion efficiency of dye sensitized solar cells.^{13,14} Recently, mesomorphic imidazolium salts were also used as new vectors for *si*-RNA transfection.¹⁵ Hence, for the further exploration of new applications and optimization of application relevant properties, the study of the self-assembly behavior, as well as the fundamental structure–property relations of ILCs^{16–32} is required.

Recently we have systematically studied the structure–property relation of a series of phenylbenzoate based rod-like imidazolium salts **C1ⁿIm–C3ⁿIm** in which the 1-phenyl-1*H*-imidazol

unit is connected with an alkoxyphenyl group through a carboxylate linking group (Scheme 1). A mesophase sequence SmA–Col_{hex}–Cub₁/*Pm3n* was observed upon decreasing the length of the *N*-terminal chain or by increasing the number and length of the *C*-terminal chains (Scheme 2).³³ The strong self-assembly tendency of such rod-like imidazolium salts prompted us to study the influence of further variations of the molecular structure.

In this contribution, the –COO– linkage in the phenylbenzoates **C1ⁿIm–C3ⁿIm** was replaced by a less polar –CH₂O– linkage and a more polar amide linkage (–CONH–), respectively, leading to two new series of rod-like and taper-shaped imidazolium salts, the ethers **E1ⁿIm–E3ⁿIm** and the amides **A1ⁿIm–A3ⁿIm**. In this notation the letters A, C and E specify the type of

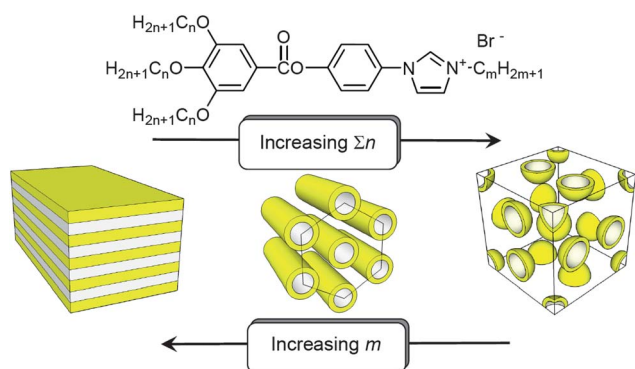


Scheme 1 Structures of reported rod-like imidazolium salts with phenylbenzoate units (“carboxylates”) **C1ⁿIm–C3ⁿIm**,³³ benzylphenylether derivatives **E1ⁿIm–E3ⁿIm** (“ethers”) and benzanilide derivatives **A1ⁿIm–A3ⁿIm** (“amides”) under investigation.

^aChemistry Department, Yunnan University, Kunming, Yunnan, 650091, P. R. China. E-mail: xhcheng@ynu.edu.cn; Fax: (+86) 871 5032905

^bInstitute of Chemistry, Organic Chemistry, Martin-Luther University Halle-Wittenberg, Kurt-Mothes Str. 2, 06120 Halle/Saale, Germany. E-mail: carsten.tschierske@chemie.uni-halle.de; Fax: (+49) 345 55 27346

† Electronic supplementary information (ESI) available. See DOI: 10.1039/c2sm06854k



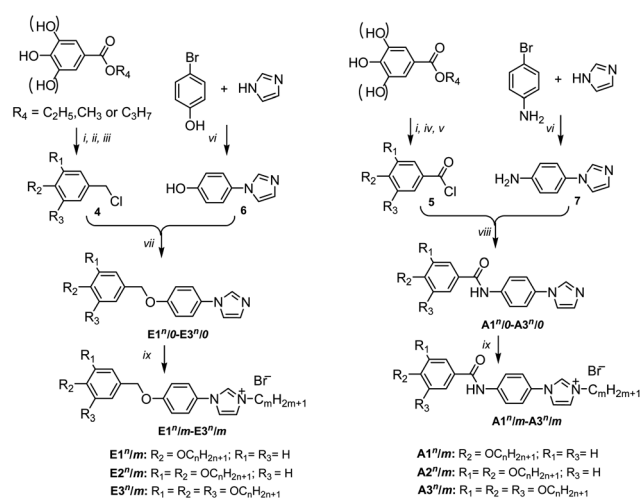
Scheme 2 Development of the mesophase structure depending on the length and number of the *C*-terminal chains and the length of the *N*-terminal chains attached to the imidazolium based rod-like core as observed for the phenylbenzoate based imidazolium salts $C1^m/m-C3^m/m$.³³

linking group (**A** = amide = $-\text{CONH}-$, **C** = carboxylate = $-\text{COO}-$ and **E** = ether = $-\text{CH}_2\text{O}-$), the next number indicates the number of alkoxy chains attached to the nonionic end of the molecule ("*C*-terminal chains"), the following superscript *n* defines the length of these chains, and the last number *m* identifies the number of carbon atoms in the *N*-terminal hydrocarbon chain attached to the imidazolium salt structure. Here "0" means that there is no alkyl chain, *i.e.* these compounds represent the nonionic precursors (1-phenyl-1*H*-imidazoles) from which the imidazolium salts were prepared by quaternization (Scheme 1). Upon decreasing the length of the *N*-terminal chain or increasing the number and length of the *C*-terminal chains, the sequence $\text{SmA}-\text{Col}_{\text{hex}}-\text{Cub}_1/\text{Pm}3n$ was found for the ether based imidazolium salts, similar to that found for the previously reported esters,³³ while only SmA and Col_{hex} phases were detected for the related amides (Scheme 4). Compared with the corresponding carboxylates **C**, the ethers **E** generally show lower phase transition temperatures and reduced mesophase stability and in most cases also reduced melting points. Both effects can be explained by the enhanced flexibility of the ether linkage. Surprisingly, the effect of the amide group is very distinct in the series of the non-charged 1*H*-Imidazoles and the corresponding imidazolium salts. Whereas the mesophases of the 1*H*-imidazoles are stabilized due to the enhanced polarity of the amide group, the mesophases of the imidazolium salts are destabilized and the interface curvature is reduced, *i.e.* micellar cubic and hexagonal columnar phases are replaced by columnar and smectic phases, respectively. It is suggested that the interaction between the amide groups and the imidazolium moieties modifies the molecular packing.

2. Results and discussion

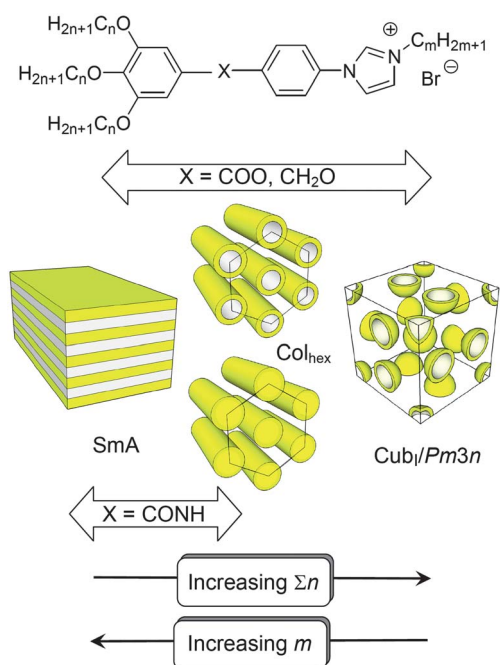
2.1. Synthesis

The synthesis of the compounds under discussion is shown in Scheme 3 (for experimental details, see the ESI†). The key step in the synthesis was an Ullman-type coupling³⁴ of 4-bromophenol or 4-bromoaniline with imidazole which gave 4-(1*H*-imidazol-1-yl)phenol **6** or 4-(1*H*-Imidazol-1-yl)aniline **7**, respectively. The



Scheme 3 Synthesis of the imidazolium bromides; Reagents and conditions: (i) C_nH_{2n+1}Br, K₂CO₃, DMF, 90 °C, overnight; (ii) LiAlH₄, THF, 50 °C, 4 h; (iii) SOCl₂, DMF, THF, 5 h; (iv) KOH, EtOH, reflux; (v) SOCl₂, DMF, THF, reflux, 5 h; (vi) K₂CO₃, CuI, DMF, N₂, reflux, 24 h; (vii) K₂CO₃, DMF, 90 °C, overnight; (viii) NaH, DMF, 90 °C, overnight; (ix) C_mH_{2m+1}Br, toluene, reflux, 16–48 h.

phenol **6** was etherified with appropriate alkoxy-substituted benzyl chlorides **4**, leading to the 1-(4-benzyloxyphenyl)-1*H*-imidazoles **E1^m/m–E3^m/m**. The amine **7** was acylated with appropriate alkoxy-substituted benzoyl chlorides **5**, leading to the 1-(4-benzamidophenyl)-1*H*-imidazoles **A1^m/m–A3^m/m**. These compounds were quaternized with appropriate *n*-alkyl bromides yielding the imidazolium based ILCs. Purification of the products was done by crystallization from methanol/chloroform (10/1) or by column chromatography; the structure and purity of



Scheme 4 Development of the mesophase structure depending on the length and number of the *C*-terminal chains and the length of the *N*-terminal chains attached to the imidazolium based rod-like aromatic core and the structure of the linking group **X**.

all compounds were confirmed by ^1H NMR and elemental analysis (see Table S3–S6, ESI†).

2.2. Investigations

The liquid crystalline properties of the synthesized compounds were studied by polarizing optical microscopy (POM, Optiphot 2, Nikon, in conjunction with a FP 82 HT heating stage, Mettler), differential scanning calorimetry (DSC, DSC-7, Perkin Elmer). The X-ray diffraction patterns of aligned or partially aligned samples were recorded with a 2D detector (HI-STAR, Siemens). Ni filtered and pin hole collimated Cu $K\alpha$ radiation was used. The exposure time was normally 60 min. The sample to detector distance was 8.8 cm and 26.9 cm for the wide angle and small angle measurements, respectively. Alignment was achieved upon slow cooling (rate: 1 K min^{-1} – 0.1 K min^{-1}) of a small droplet of the sample on a glass plate and takes place at the sample–glass or at the sample–air interface, with domains fiber-like disordered around an axis perpendicular to the interface. The aligned samples were held on a temperature-controlled heating stage. The X-ray beam was parallel to the substrate.

2.3. Liquid crystalline properties of the nonionic imidazole derivatives

The phase transition temperatures and enthalpies of the nonionic 1*H*-imidazoles with ether linking units (**E1ⁿ/0**–**E3ⁿ/0**) and amide units (**A1ⁿ/0**–**A3ⁿ/0**) are collected in Tables 1 and 2, respectively. Single chain ether derivatives exhibit monotropic smectic A phases if the alkyl chain length is at least $n = 16$ (**E1¹⁶/0** and **E1¹⁸/0**), whereas all two- and three-chain ether derivatives are not liquid crystalline. For the amide derivative the required alkyl chain length is reduced to $n = 12$ and enantiotropic SmA mesophases are observed (**A1¹²/0**, **A1¹⁶/0** and **A1¹⁸/0**). Although most of the two- and three-chain amides are crystals, one of these amides with three dodecyloxy chains (**A3¹²/0**) exhibits a monotropic

mesophase (M, see Table 2 and Fig. 1b) which is most likely a columnar phase. The amide group increases the polarity of the rod-like core and introduces the possibility of intermolecular hydrogen bonding, which both should be responsible for the formation of the stable SmA phases of the single chain nonionic amide derivatives and the occurrence of LC behavior (M) in one of the three-chain amides. However, due to crystallization this mesophase M could not be investigated in more detail.

The SmA phases were identified by polarizing microscopy by their typical appearance consisting of focal-conics, fan-like textures and pseudoisotropic regions with oily streaks, depending on the alignment conditions (see Fig. 1a, 2b). The pseudoisotropic regions indicate an on average orthogonal organization of the molecules with respect to the layer planes.³⁵

The SmA phases of the shortest and longest LC amides **A1¹²/0** and **A1¹⁸/0** were additionally investigated by X-ray scattering of aligned samples (Table 3, Table S1†). The diffraction patterns show strong fundamental layer reflections on the meridian along with diffuse outer scatterings with intensity maxima on the equator (Fig. 2a, Fig. S3†). This confirms layer structures in which the long axes of the molecules are on average parallel to the layer normal. The maxima of the outer diffuse scattering at $d = 0.46$ – 0.47 nm correspond to the average lateral distances between the molecules in the fluid LC state. Compared with the molecular length in the most stretched conformations ($L = 2.9$ nm for **A1¹²/0** and $L = 3.9$ nm for **A1¹⁸/0**³⁶), the layer spacings ($d = 3.9$ and 4.7 nm, respectively) are larger than the molecular lengths ($d/L = 1.2$ – 1.3 , see Table 3), but significantly smaller than twice the lengths, indicating bilayer structures with complete interdigitation of the alkyl chains (SmA₂) as shown in Fig. 3.³⁷

This is the same phase structure as previously reported for related 1-phenyl-1*H*-imidazoles incorporating ester linkages (**C1ⁿ/0**)³³ and therefore it is likely that formation of this type of interdigitated bilayer structure is a general feature of single chain 1-phenyl-1*H*-imidazoles, independent from the linking group.

Table 1 Mesophases, transition temperatures and transition enthalpy values of the 1-phenyl-1*H*-imidazoles **E1ⁿ/0**–**E3ⁿ/0** with an ether linking group^a

Comp	R ₁	R ₂	R ₃	$T/^\circ\text{C}$ [$\Delta H/\text{kJ mol}^{-1}$]	f_{RC}
E1⁶/0	H	OC ₆ H ₁₃	H	Cr 112 [32.2] Iso	0.34
E1¹²/0	H	OC ₁₂ H ₂₅	H	Cr 126 Iso ^b	0.49
E1¹⁶/0	H	OC ₁₆ H ₃₃	H	Cr 111 [68.7] (SmA ₂ 91 [8.5] ^c) Iso	0.56
E1¹⁸/0	H	OC ₁₈ H ₃₇	H	Cr 109 [61.7] (SmA ₂ 89 [3.1] ^c) Iso	0.59
E2¹⁶/0	OC ₁₆ H ₃₃	OC ₁₆ H ₃₃	H	Cr 92 [89.9] Iso	0.72
E3¹²/0	OC ₁₂ H ₂₅	OC ₁₂ H ₂₅	OC ₁₂ H ₂₅	Cr 43 [36.1] Iso	0.75
E3¹⁴/0	OC ₁₄ H ₂₉	OC ₁₄ H ₂₉	OC ₁₄ H ₂₉	Cr 59 [91.4] Iso	0.78
E3¹⁶/0	OC ₁₆ H ₃₃	OC ₁₆ H ₃₃	OC ₁₆ H ₃₃	Cr 71 [109.8] Iso	0.80
E3¹⁸/0	OC ₁₈ H ₃₇	OC ₁₈ H ₃₇	OC ₁₈ H ₃₇	Cr 80 [115.1] Iso	0.82

^a Transition temperatures and enthalpy changes (in square brackets) were determined by DSC (peak temperature, first heating scan, $10^\circ\text{C min}^{-1}$), values in round parentheses indicate monotropic (metastable) phases, abbreviations: Cr = crystalline solid, N = nematic phase, SmA₂ = smectic A phase with interdigitated double layer structure,³⁷ Iso = isotropic liquid state; f_{RC} = volume fraction of the C-terminal alkyl chains R₁–R₃ including the ether oxygens. ^b Transition temperature was determined by POM. ^c Phase transitions observed on cooling.

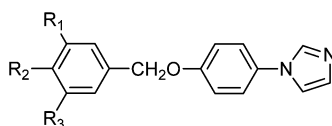
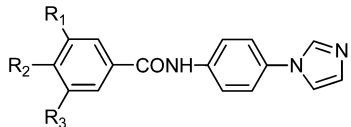


Table 2 Mesophases, transition temperatures, and transition enthalpy values of the 1-phenyl-1*H*-imidazoles **A1ⁿ/0**–**A3ⁿ/0** with amide linking groups^a


Comp	R ₁	R ₂	R ₃	T ^o C [ΔH /kJ mol ⁻¹]	f _{RC}
A1⁶/0	H	OC ₆ H ₁₃	H	Cr 148 [33.4] Iso	0.34
A1¹²/0	H	OC ₁₂ H ₂₅	H	Cr 132 [42.1] SmA ₂ 169 [3.6] Iso	0.49
A1¹⁶/0	H	OC ₁₆ H ₃₃	H	Cr 129 [40.3] SmA ₂ 183 [3.8] Iso	0.56
A1¹⁸/0	H	OC ₁₈ H ₃₇	H	Cr 127 [49.5] SmA ₂ 184 [4.4] Iso	0.59
A2¹⁶/0	OC ₁₆ H ₃₃	OC ₁₆ H ₃₃	H	Cr 136 [51.3] Iso	0.72
A3⁶/0	OC ₆ H ₁₃	OC ₆ H ₁₃	OC ₆ H ₁₃	Cr 62 [19.2] Iso	0.61
A3¹⁰/0	OC ₁₀ H ₂₁	OC ₁₀ H ₂₁	OC ₁₀ H ₂₁	Cr 72 [55.6] Iso	0.72
A3¹²/0	OC ₁₂ H ₂₅	OC ₁₂ H ₂₅	OC ₁₂ H ₂₅	Cr 58 [62.9] (M 24 [0.5] ^b) Iso	0.75
A3¹⁴/0	OC ₁₄ H ₂₉	OC ₁₄ H ₂₉	OC ₁₄ H ₂₉	Cr 67 [79.2] Iso	0.78
A3¹⁸/0	OC ₁₈ H ₃₇	OC ₁₈ H ₃₇	OC ₁₈ H ₃₇	Cr 86 [100.5] Iso	0.82

^a Transition temperatures and enthalpy changes (in square brackets) were determined by DSC (peak temperature, first heating scan, 10 °C min⁻¹), values in round parentheses indicate monotropic (metastable) phases, abbreviations: M = unknown mesophase most probably a columnar phase according to textural observations (Fig. 1b); for other abbreviations, see Table 1. ^b Phase transition observed on cooling.

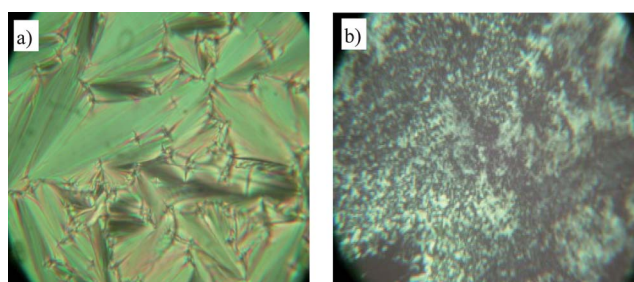


Fig. 1 Representative textures as seen between crossed polarizers: (a) SmA₂ phase of compound **A1¹⁶/0** at $T = 182$ °C and (b) M phase of compound **A3¹²/0** at $T = 24$ °C.

Table 3 Comparison of the XRD data of the SmA phases and the molecular dimensions of the single chain 1-phenyl-1*H*-imidazoles **A1ⁿ/0** with those of the imidazolium bromides **E1ⁿ/m^a**

Comp	R ¹	R ²	R ¹	<i>m</i>	<i>d</i> /nm (T /°C)	<i>L</i> /nm	<i>d</i> / <i>L</i>
A1¹²/0	H	OC ₁₂ H ₂₅	H	—	3.9 (165)	2.9	1.3
A1¹⁸/0	H	OC ₁₈ H ₃₇	H	—	4.7 (140)	3.9	1.2
E1¹²/4	H	OC ₁₂ H ₂₅	H	4	5.9 (80)	3.4	1.7
E1¹²/12	H	OC ₁₂ H ₂₅	H	12	4.0 (100)	4.6	0.9

^a Abbreviations: *d* = layer spacing; *L* = molecular length measured between the ends of the terminal chains and assuming a most stretched conformation with all-*trans* conformation of the alkyl chains;³⁶ for details see Fig. 5, S3,S4 and Table S1.

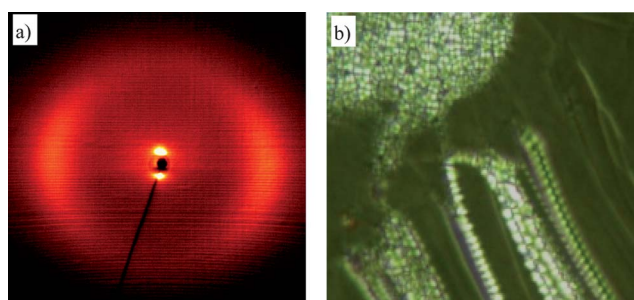


Fig. 2 Compound **A1¹²/0**: (a) X-ray diffraction pattern of an aligned sample of the SmA₂ phase at $T = 165$ °C; (b) oily streaks texture (between crossed polarizers) at the same temperature (dark areas represent homeotropically aligned regions).

For the mesophase stability the order is ether < ester < amide, which is in line with the increasing polarity of the linking groups.

2.4. Liquid crystalline properties of the ionic imidazolium salts

In contrast to the series of non-charged imidazoles **E1ⁿ/0**–**E3ⁿ/0**, in the series of the ether based imidazolium bromides **E1ⁿ/m**–**E3ⁿ/m**

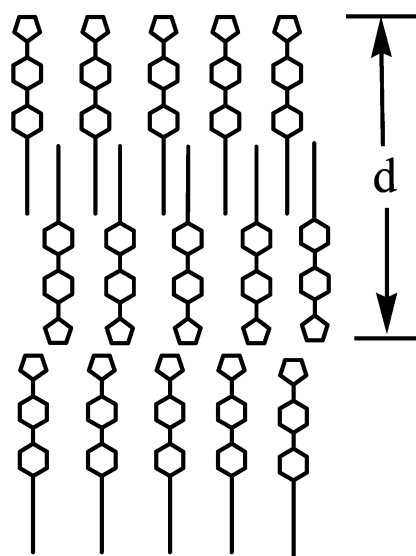


Fig. 3 Model of the structure of the SmA phases³⁸ of compounds **A1ⁿ/0** (SmA₂).^{33,37}

a variety of different LC phases including smectic phases, columnar and cubic phases is found. The amide based imidazolium bromides **A1^m–A3^m** have much higher melting points and only smectic and columnar mesophases could be observed.

2.4.1 Imidazolium bromides with a single C-terminal chain.

The transition temperatures of the synthesized single chain imidazolium bromides incorporating amide and ether linking units are collected in Table 4, together with related compounds incorporating ester linkages.³³ All these compounds can be regarded as typical rod-like ionic liquid crystals (ILCs) because they all have two flexible chains, one at each end of the rod-like aromatic core. The melting temperatures strongly increase in the order ether < ester < amide where the difference in melting temperature between each class of compounds is about nearly 100 K. The amide derivatives **A1^m** are all crystals with very high melting points and no LC phases can be observed for these compounds.

In contrast, broad regions of SmA phases (for representative textures see Fig. 4 and Fig. S1a, ESI†) were found for the ethers **E1^m**. Their stability increases with growing total alkyl chain length ($m + n$). Though the stability of the SmA phases is reduced by replacing the $-\text{COO}-$ group by the $-\text{CH}_2\text{O}-$ group, the reduction of the melting point is much larger. This makes the ethers **E1^m**, having melting points between 43 and 87 °C and mesophase ranges of up to 160 K, the most useful smectic ILC in this series.

The layer spacing of compound **E1²/4** with a short *N*-terminal chain ($d = 5.9$ nm, as determined by XRD) is larger than the molecular length ($L = 3.4$ nm, $d/L = 1.7$) but smaller than twice the length (Table 3), indicating a bilayer structure with

Table 4 Mesophases, transition temperatures, and transition enthalpy values of the single chain imidazolium bromides **E1^m** and **A1^m** incorporating ether and amide linkages in comparison with the related imidazolium bromides **C1^m**³³ with ester linking units^a

Compd	X	n	m	$T/^\circ\text{C}$ [$\Delta H/\text{kJ mol}^{-1}$]
E1²/3	CH ₂ O	12	3	Cr 43 [15.2] SmA ₂ 139 [1.9] Iso
E1²/4	CH ₂ O	12	4	Cr 81 [13.0] SmA ₂ 174 Iso ^b
E1²/12	CH ₂ O	12	12	Cr 87 [28.7] SmA ₁ 212 Iso (dec.)
E1⁴/12	CH ₂ O	14	12	Cr 60 [32.7] SmA ₁ 224 Iso (dec.)
E1⁶/3	CH ₂ O	16	3	Cr 52 [21.2] SmA ₂ 213 [0.7] Iso
E1⁶/6	CH ₂ O	18	6	Cr 68 [35.2] SmA 216 Iso (dec.)
C1²/4^c	COO	12	4	Cr 151 [15.1] SmA ₂ 196 Iso (dec.)
C1²/12^c	COO	12	12	Cr 169 [23.5] SmA ₁ > 200 Iso (dec.)
C1⁶/6^c	COO	18	6	Cr 156 [22.4] SmA > 200 Iso (dec.)
A1²/4	CONH	12	4	Cr 246 [32.6] Iso (dec.)
A1⁶/4	CONH	16	4	Cr 242 [42.1] Iso (dec.)

^a Transition temperatures and enthalpy changes (in square brackets) were determined by DSC (peak temperature, first heating scan, 10 K min⁻¹; no transition enthalpies are given for clearing temperatures associated with decomposition), abbreviations: SmA₁ = SmA phase with monolayer structure; SmA = SmA phase with unknown layer periodicity; for the other abbreviations, see Table 1. ^b Transition temperature were determined by POM (Fig. 4a). ^c See ref. 33.

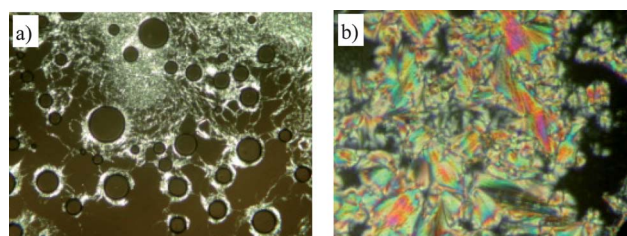


Fig. 4 Representative textures of SmA phases as seen between crossed polarizers: (a) for **E1²/4** at $T = 170$ °C (SmA₂) with predominately homeotropic alignment (dark regions) and oily streaks, and (b) for **E1⁶/6** at $T = 185$ °C (SmA) with predominately homogeneous alignment (fan-like texture).

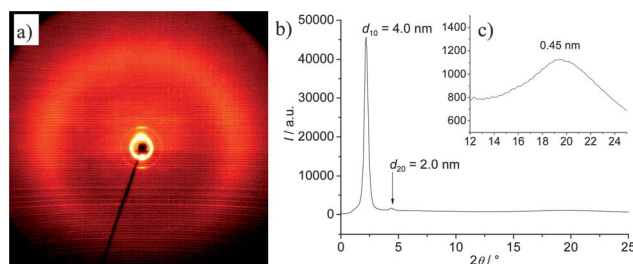


Fig. 5 (a) XRD pattern of a partly aligned sample of the SmA phase of compound **E1²/12** at $T = 100$ °C; (b) 2θ -scan over this diffraction pattern, and (c) enlarged wide angle region (the lower part of the XRD pattern is shaded by the heating stage).

interdigitation of the short *N*-alkyl chains and the long *C*-alkyl chains in distinct, separate layers (SmA₂ phase, Fig. 6a).³⁷ In this SmA₂ phase there is a parallel-side-by-side packing of the aromatic cores, allowing the segregation of the polar imidazolium units from the less polar alkoxy-substituted benzene rings at the opposite end.

The layer spacing ($d = 4.0$ nm) of compound **E1²/12** with two long terminal chains is a bit smaller than the molecular length³⁶ ($L = 4.6$ nm, $d/L = 0.9$, see Table 3), indicating a monolayer structure as shown in Fig. 6b, where the *N*-terminal and *C*-terminal chain are mixed in common layers. In the resulting monolayer structure there is an on average antiparallel side-by-side packing of the aromatic units which is favored for entropic reasons. The difference between L and d in the single layer structure might be a consequence of a relatively low order parameter of the aromatics and alkyl chains due to the presence of a distortion caused by the bulky bromide counter ions.

2.4.2 Imidazolium bromides with two and three C-terminal chains. Table 5 shows that for compounds with a short *N*-terminal chain ($m = 3$) by increasing the number of *C*-terminal chains (C_{16}) from one to three a transition from SmA via a hexagonal columnar phase (Col_{hex}) to a cubic phase (Cub) takes place. As the volume fraction of the *C*-terminal hydrocarbon chains (f_{RC}) increases on going from **E1⁶/3** to **E3⁶/3** the curvature of the aromatic–aliphatic interface increases and therefore the cubic phase of **E3⁶/3** should represent a discontinuous (micellar) cubic phase (Cub₁).^{33,39} This is in line with the XRD diffraction pattern obtained for the cubic phase of

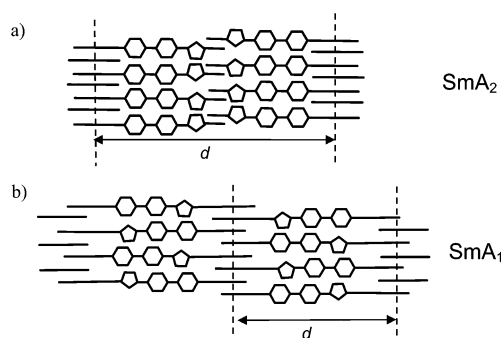


Fig. 6 Schematic sketches showing (a) the organization of single chain imidazolium salts in an interdigitated double layer SmA_2 phase ($d > L$) and (b) in a monolayer SmA_1 phase ($d < L$).³³

Table 5 Effect of increasing the number of *C*-terminal alkyl chains on the properties of ether based imidazolium salts^a

Compd	R ₁	R ₂	R ₃	<i>T</i> ^o C [Δ <i>H</i> /kJ mol ⁻¹]	<i>f</i> _{RC}
E1¹⁶/3	R	H	H	Cr 52 [21.2] SmA 213 [0.7] Iso	0.48
E2¹⁶/3	R	R	H	Cr 72 [41.0] Col _{hex} 242 [5.2] Iso	0.65
E3¹⁶/3	R	R	R	Cr 89 [34.7] Cub _I 184 [0.7] Iso	0.74

^a R = OC₁₆H₃₃.

compound **E3¹⁶/3**, which can be indexed on a $Pm3n$ lattice (see below) and the $Pm3n$ lattice is known to be the most favoured for thermotropic micellar cubic phases.^{39–43} A similar phase sequence $\text{SmA} - \text{Col}_{\text{hex}} - \text{Cub}_I$ is observed if f_{RC} is related to the observed phase structures for a broader range of molecules as shown in Fig. 7 for compounds with $m = 3$. In this series SmA phases were found for $f_{\text{RC}} < 0.5$, Col_{hex} phases occur between $f_{\text{RC}} = 0.6$ and 0.72 and for $f_{\text{RC}} > 0.72$ Cub_I phases were found.

In the series of ether based imidazolium salts **E3¹⁴/m** with three *C*-terminal chains only slight elongation of the *N*-terminal chain

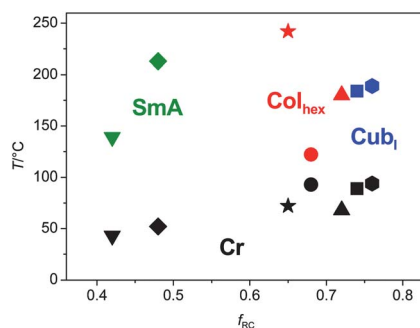


Fig. 7 Plot of phase transition temperatures and phase types (indicated by color) against the volume fraction of the *C*-terminal chains (f_{RC}) for compounds (▼) = **E1¹²/3**, (◆) = **E1¹⁶/3**, (★) = **E2¹⁶/3** (●) = **A3¹²/3**, (▲) = **E3¹⁴/3**, (■) = **E3¹⁶/3**, (hexagons) = **E3¹⁸/3**.

from $m = 2$ to $m = 5$, corresponding to an increase of the volume fraction of the *N*-terminal chains f_{RN} from 0.04 to about 0.10 (see Fig. 8), leads to a phase sequence $\text{Cub}_I - \text{Col}_{\text{hex}} - \text{SmA}$, *i.e.* in this way at first the cubic and then also the Col_{hex} phase is removed. In the same order also the mesophase stability is significantly reduced, so that for some compounds with $m = 5, 6$ the SmA phases become monotropic or cannot be investigated due to rapid crystallization. All ether based imidazolium salts have lower transition temperatures than the ester based imidazolium salts due to the increased molecular flexibility and reduced polarity of the $-\text{CH}_2\text{O}-$ linkage.⁴⁴ The effect on mesophase stability is larger than on the melting points, leading to smaller mesophase ranges for the ether based imidazolium salts. Nevertheless, the lower transition temperatures make them advantageous over the previously reported esters **C3¹/m** as the mesomorphic temperature range is shifted to lower temperatures and hence, thermal decomposition in the mesophase region is avoided.

The effect of increasing the length of the *C*-terminal chains on the mesophase morphology and mesophase stability is much smaller; nevertheless Col_{hex} phases can be replaced by Cub_I phases upon elongation of the *C*-terminal chain (compare compounds **E3¹⁴/3**– Col_{h} and **E3¹⁶/3**– Cub_I in Fig. 7).

In a series of related amides **A3¹/m** only the phase sequence $\text{SmA} - \text{Col}_{\text{hex}}$ is observed upon elongation of the *N*-terminal chain, but the Cub_I phases are missing for these compounds (Table 6, bottom). Besides the more limited variety of different mesophases, the melting points of the amide based imidazolium salts are significantly enhanced compared to the related esters and ethers and the stability of the mesophases is reduced (compare **E3¹⁶/2** and **A3¹⁶/2** as examples).

Hexagonal columnar phases. The textures of the columnar mesophases, as observed by POM, are characterized by typical spherulitic domains as shown in Fig. 9a,c. These columnar phases are optically uniaxial as indicated by the completely dark appearance of regions with homeotropic alignment of the columns (columns perpendicular to the glass substrates) and they are optically negative as indicated by investigation with a λ -retarder plate (Fig. 9b,d). This means that in the columns the preferred direction of the intramolecular π -conjugation pathway (*i.e.* the long axis of the rod-like aromatic cores) is on average perpendicular to the column long axis.

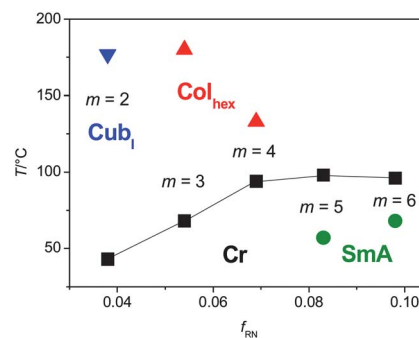


Fig. 8 Plot of phase transition temperatures and phase types (indicated by color) against the volume fraction of the *N*-terminal chains (f_{RN}) for the series of compounds **E1¹⁴/m**.

Table 6 Mesophases, transition temperatures and transition enthalpy values of the three-chain imidazolium bromides **E3ⁿm** and **A3ⁿm^d**

Comp	X	n	m	<i>T</i> ^o C [ΔH /kJ mol ⁻¹]	<i>f</i> _{RC}
E3¹²/4	CH ₂ O	12	4	Cr 91 [51.7] Col _h 109 [0.56] Iso	0.68
E3¹²/5	CH ₂ O	12	5	Cr 98 [37.2] (SmA 84 [0.38]) Iso	0.66
E3¹⁴/2	CH ₂ O	14	2	Cr 43 [61.8] Cub _I 177 ^{b,c} Iso	0.73
E3¹⁴/3	CH ₂ O	14	3	Cr 68 [101] Col _h 180 [0.2] Iso	0.72
E3¹⁴/4	CH ₂ O	14	4	Cr 94 [65.6] Col _{hex} 133 [0.48] Iso	0.71
E3¹⁴/5	CH ₂ O	14	5	Cr 98 [33.2] (SmA ^b 57 [0.31]) Iso	0.70
E3¹⁴/6	CH ₂ O	14	6	Cr 96 [32.6] (SmA ^b 68 [0.27]) Iso	0.68
E3¹⁶/2	CH ₂ O	16	2	Cr 96 [61.6] Cub _I 217 ^{b,c} Iso	0.75
E3¹⁶/3	CH ₂ O	16	3	Cr 89 [35.0] Cub _I 184 [0.66] Iso	0.74
E3¹⁶/4	CH ₂ O	16	4	Cr 100 [78.7] Cub _I 100 ^d Col _h 148 [0.33] Iso	0.73
E3¹⁶/5	CH ₂ O	16	5	Cr 97 [32.7] Iso	0.72
E3¹⁸/3	CH ₂ O	18	3	Cr 94 [67.2] Cub _I 189 [1.9] Iso	0.76
E3¹⁸/5	CH ₂ O	18	5	Cr 92 [20.5] Iso	0.74
A3¹²/2	CONH	12	2	Cr 77 [16.6] Col _h 183 [0.18] Iso	0.70
A3¹²/3	CONH	12	3	Cr 93 [31.9] Col _{hex} 122 [0.37] Iso	0.68
A3¹⁶/2	CONH	16	2	Cr 115 [62.3] Col _h 189 [0.44] Iso	0.75
A3¹⁶/4	CONH	16	4	Cr 127 [28.0] (SmA ^b 92 [0.34]) Iso	0.73

^a Transition temperatures and enthalpy changes (in square brackets) were determined by DSC (peak temperature, first heating scan, 10 °C min⁻¹), abbreviations: Col_{hex} = hexagonal columnar phase as confirmed by XRD; Col_h = hexagonal columnar phase (assignment based only on optical investigations, no XRD performed or only 01-reflection in non-aligned sample observed); Cub_I = cubic mesophase, most probably Cub_I/Pm3n = micellar cubic mesophase with space group Pm3n; for other abbreviations, see Table 1. ^b Determined by POM. ^c No peak could be found for this transition in the DSC traces, probably due to slow transition and partial decomposition at the transition temperature. ^d Phase transitions observed on heating, on cooling Col_{hex} 95 Cub_I.

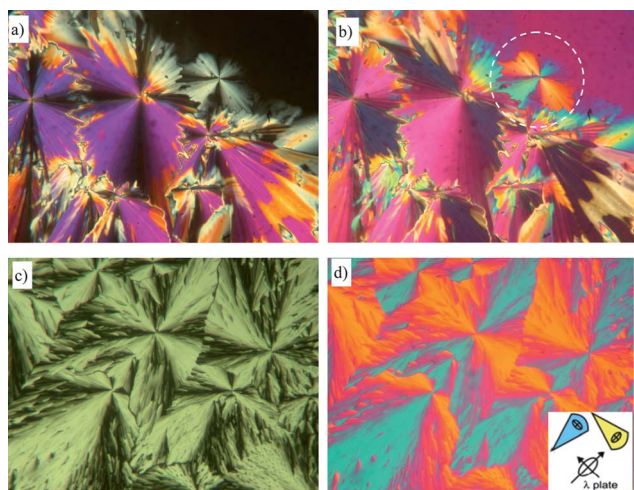


Fig. 9 Typical textures (crossed polarizers) of the Col_{hex} phases of the imidazolium bromides: (a) compound **A3¹⁶/2** at 180 °C (dark area at the right top is a homeotropically aligned region); (b) same region with λ -retarder plate and (c) **E3¹⁶/4** at 120 °C; (d) same region with λ -retarder plate, the inset shows the indicatrix orientation in the λ -compensator.

XRD investigations (see Table 7, S1 and S2) show two or three small angle reflections with a ratio of their reciprocal spacing 1 : 3^{1/2} or 1 : 3^{1/2} : 2 which can be indexed to the 10, 11 (and 20) reflections of a hexagonal lattice (Fig. 10, S5, S6). In some cases only the 10 reflection can be observed which in the 2D diffraction pattern of oriented samples is splitted into 6 spots on a regular

hexagon, confirming a hexagonal columnar mesophase (Fig. 10 and S6). The hexagonal lattice parameter is $a_{\text{hex}} = 6.1$ nm for **E2¹⁶/3** with only two C-terminal chains. For the compounds with three chains it is around 5.0 nm for the ethers and between 4.3–4.6 nm for the amides (see Table 7). Though not for all columnar phases XRD has been carried out, based on textural similarities, it is very likely that also the other columnar phases (indicated as Col_h in Table 6) represent Col_{hex} phases. The number of molecules organized in a slice of the columns with a height of $h = 0.45$ nm (maximum of the diffuse wide angle scattering) were

Table 7 Comparison of XRD data and molecular dimensions of the columnar and cubic phases of imidazolium bromides with three C-terminal chains^a

Comp	<i>n</i>	<i>m</i>		<i>a</i> /nm (<i>T</i> ^o C)	<i>n</i>
E2¹⁶/3	16	3	Col _{hex} /p6mm	6.1 (100)	10.3
E3¹²/4	12	4	Col _{hex} /p6mm	4.9 (100)	6.0
E3¹⁴/4	14	4	Col _{hex} /p6mm	4.9 (120)	5.5
E3¹⁶/3	16	3	Cub _I /Pm3n	10.6 (120)	80
E3¹⁶/4	16	4	Col _{hex} /p6mm	5.1 (120)	5.5
			Cub _I /Pm3n	10.8 (100)	83
A3¹²/2	12	2	Col _{hex} /p6mm	4.3 (140)	4.8
A3¹⁶/2	16	2	Col _{hex} /p6mm	4.6 (140)	4.5

^a Abbreviations: *a* = lattice parameter determined by XRD (a_{hex} and a_{cub} , respectively); *n* = number of molecules in the cross section of a column in the Col_{hex} phases (with assumed height of 0.45 nm)/ respective number of molecules in each micelle of the cubic/Pm3n lattice ($n_{\text{cell}}/8$).

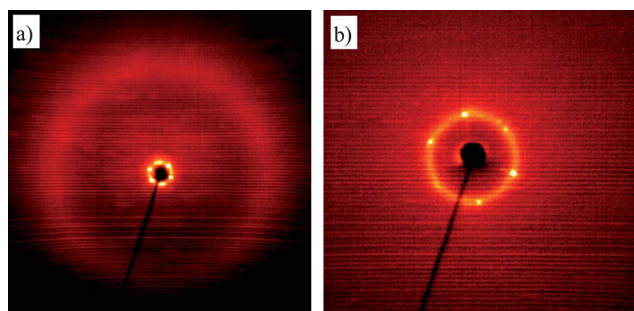


Fig. 10 X-Ray diffraction pattern of the Col_{hex} phase of compound **E3¹⁶/4** at $T = 120$ °C, (a) wide angle pattern and (b) small angle pattern (the lower part is shaded by the heating stage).

estimated using eqn (1) and assuming a density of $\rho = 1 \text{ g cm}^{-3}$ (N_A = Avogadro constant; M = molecular mass, see also Table 7 and S2). This number decreases from $n = 10$ for the two-chain ether **E2¹⁶/3** to $n = 5.5$ – 6.0 for the investigated three-chain ethers **E3ⁿ/m** and to $n = 4.5$ – 4.8 for the corresponding three chain amides **A3ⁿ/m**.

$$n = (a^2/2)\sqrt{3}h(N_A/M)\rho \quad (1)$$

Based on the results of optical investigations, XRD, the development of phase type and lattice parameters depending on the chain lengths and also considering the results obtained for the related carboxylates **C3ⁿ/m**,³³ the following model could be deduced for the organization of the molecules in the columnar phases. Accordingly, in the Col_{hex} phases the short *N*-terminal alkyl chains form a lipophilic core, which is surrounded by a polar stratum of the ionic parts and aromatic units (Fig. 11). These core-shell cylinders are assembled in the lipophilic continuum of the *C*-terminal alkyl chains on a hexagonal lattice. This kind of organization allows a complete segregation of the incompatible units, each in its own domain, and it requires an interdigitation of the *C*-terminal alkyl chains of molecules in adjacent columns to completely fill the space in the lipophilic periphery. The effective diameters of the columns (considering this interdigitation) correspond to the experimentally observed hexagonal lattice parameters a_{hex} . The large decrease of the number of molecules organized in the cross section of the columns, observed with increasing number of *C*-terminal chains is due to the increase of the taper angle with rising space requirement of the *C*-terminal chains.

In the proposed arrangements the space available for the packing of the *N*-terminal alkyl chain at the apex of the taper shaped molecules in the middle of the column cores is strongly limited and only slight enlargement of these chains causes the columns to burst. This is thought to be the reason for the strong decrease of the stability of the Col phases upon slight elongation of the *N*-terminal chains by only one CH₂ group (compare, for example, **E3¹⁴/3** and **E3¹⁴/4** in Table 6) and the transition to SmA phases, or even the loss of LC phases upon further elongation of this chain.

Cubic phases. For the triple chain ether-based imidazolium bromides **E3ⁿ/m** with very short *N*-terminal chains ($m = 2, 3, 4$) and three relatively long *C*-terminal chains ($n = 14, 16, 18$)

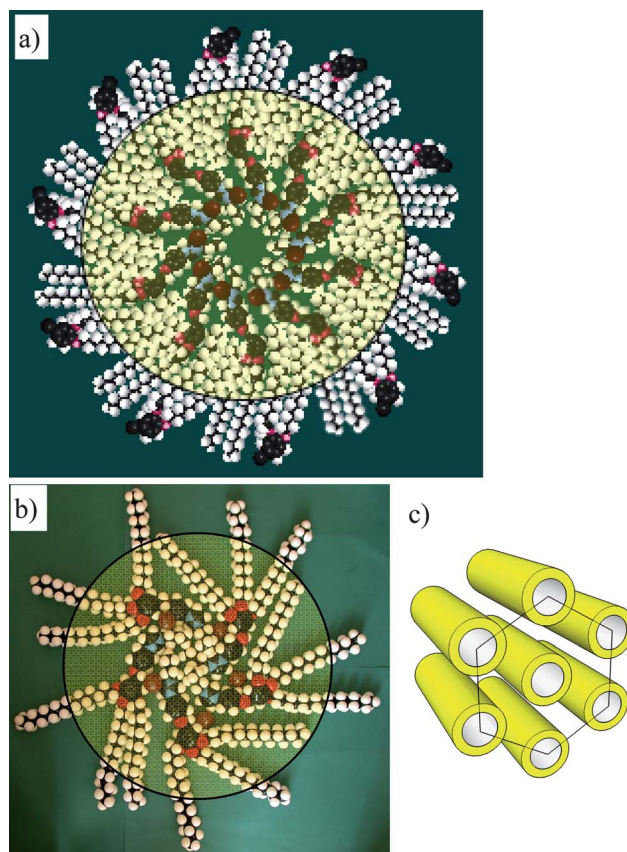


Fig. 11 Models showing schematically the molecular organization in the Col_{hex} phases: (a) cross section through a single column of the Col_{hex} phase of the two-chain compound **E2¹⁶/3**, further improved space filling in the middle would be obtained by more disorder, as shown in (b); (b) cross section through a single column of the Col_{hex} phase of the three-chain compound **E3¹⁶/4**; in both cases a dense packing in the periphery is achieved by interdigitation with the chains of adjacent columns (as shown in (a), but not in (b)); the yellow regions show the dimensions provided by the experimentally observed hexagonal lattice parameters; brown spheres represent the bromide counter ions; (c) shows the arrangement of the columns on a hexagonal lattice.

optically isotropic mesophases were observed, which are not fluid, but represent soft solids with viscoelastic response on shear forces, as typical for cubic mesophases.⁴⁵ The compounds **E3ⁿ/2** and **E3ⁿ/3** (with $n = 14, 16, 18$) form the cubic phase in the whole mesomorphic temperature range, whereas compound **E3¹⁶/4** represents a special case which forms the cubic phase below a Col_{hex} phase (Table 7, S1, S2 and Fig. 12).

The isotropic mesophases of compounds **E3¹⁶/3** and **E3¹⁶/4** were investigated by XRD. The diffraction patterns are characterized by a diffuse scattering in the wide-angle region, indicating the fluid LC state. The positions of the sharp spot-like reflections in the small-angle region are in line with a cubic lattice with $Pm\bar{3}n$ space group (see Table 7–9, S1, S2 and Fig. S7, S8†). The calculated lattice parameter is $a_{\text{cub}} = 10.6 \text{ nm}$ for **E3¹⁶/3** and $a_{\text{cub}} = 10.8 \text{ nm}$ for **E3¹⁶/4**. The $Pm\bar{3}n$ lattice is the most commonly observed lattice for micellar cubic phases (Cub₁) occurring in systems formed by spheroidal aggregates with soft corona.^{46,47} In this type of phase the molecules are organized in closed spheroidal aggregates and there are 8 of these aggregates

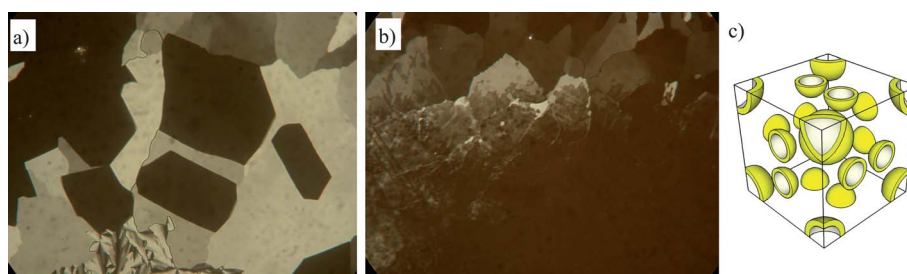


Fig. 12 Texture of the Cub_I phase of compound **E3¹⁶/4** (dark areas) (a) growing from the hexagonal columnar mesophase (bright areas) on cooling at $T = 95\text{ °C}$ and (b) $\text{Cub}_I\text{-Col}_{\text{hex}}$ transition on heating at $T = 100\text{ °C}$; (c) shows a model of the arrangement of the spheroidal aggregates in the Cub_I phase with $Pm\bar{3}n$ lattice (the interior of the spheroids is filled by the N -terminal alkyl chains, the continuum is formed by the C -terminal alkyl chains).

in each unit cell which have, depending on their crystallographic position, a slightly different shape.^{39,41,47}

For the investigated compounds each micelle is built up of approximately 80–83 molecules (see Table 7 and S2). Considering the molecular structure, these cubic phases can be regarded as micellar cubic phases (Cub_I phases), where spheroids (short column segments^{39c}) incorporating the short N -terminal chains, the imidazolium units, bromide ions and aromatic cores adopt fixed positions on a long range cubic $Pm\bar{3}n$ lattice in a continuum of the fluid and partly interdigitated C -terminal alkyl chains (Fig. 12c). As already proposed for the ester based imidazolium salts and confirmed by the experimental observations made here, the spheroids should have a core–shell structure with aliphatic cores formed by the short N -terminal chains in closed shells formed by the charged units and the rod-like cores (Fig. 12c). This packing is only possible if the N -terminal chains are very short, so that they can be accommodated in the cores of the spheroids and do not significantly disturb the packing of the polar imidazolium salt units. Only slight elongation of the N -terminal chains distorts this arrangement and the closed spheroidal micelles burst and are replaced at first by infinite columns and finally by layers. Beside this steric effect, elongation of the N -terminal chains also allows these chains to mix with the longer C -terminal chains more easily. This favors an antiparallel side-by-side packing of the molecules (as in the SmA_1 phases of the related compounds with only one C -terminal chain, see section 2.4.1) and in this way additionally increases the steric disturbance caused by these chains. For this reason the phase sequence $\text{Cub}_I\text{-Col}_{\text{hex}}\text{-SmA}$ is observed by elongation of the N -terminal chain by only 2–3 CH_2 groups (see Fig. 8), whereas the effect of the length of the C -terminal chain on mesophase type is only moderate (see Fig. 7).

Table 8 Crystallographic data of the $Pm\bar{3}n$ cubic phase ($a = 10.6\text{ nm}$) of **E3¹⁶/3** at 120 °C .^a

$\theta_{\text{obs}}/\text{°}$	d_{obs}/nm	hkl	$d_{\text{calc}}/\text{nm}$	$d_{\text{obs}} - d_{\text{calc}}$
0.83	5.36	200 ($\sqrt{4}$)	5.28	0.08
0.94	4.72	210 ($\sqrt{5}$)	4.72	0.00
1.03	4.29	211 ($\sqrt{6}$)	4.31	-0.02
1.53	2.88	320 ($\sqrt{13}$)	2.92	-0.04
1.89	2.34	420 ($\sqrt{20}$)	2.36	0.02

^a θ_{obs} = experimental scattering angles; d_{obs} = experimental and d_{calc} = calculated d spacing; hkl = assigned indices.

Table 9 Crystallographic data of the $Pm\bar{3}n$ cubic phase ($a = 10.8\text{ nm}$) of **E3¹⁶/4** at 100 °C .^a

$\theta_{\text{obs}}/\text{°}$	d_{obs}/nm	hkl	$d_{\text{calc}}/\text{nm}$	$d_{\text{obs}} - d_{\text{calc}}$
0.83	5.33	200 ($\sqrt{4}$)	5.38	-0.05
0.92	4.81	210 ($\sqrt{5}$)	4.81	0.00
1.00	4.40	211 ($\sqrt{6}$)	4.39	0.01
1.51	2.92	320 ($\sqrt{13}$)	2.98	-0.06
1.83	2.41	420 ($\sqrt{20}$)	2.41	0.00

Compound **E3¹⁶/4** has a cubic phase which forms slowly on cooling the Col_{hex} phase to $T = 95\text{ °C}$ (Fig. 12a) whereas the phase transition of the Cub phase to the Col_{hex} phase on heating takes place at $T = 100\text{ °C}$ (Fig. 12b). This hysteresis is typical for cubic phases^{45b} and the $Pm\bar{3}n$ space group was confirmed by XRD (Table S1, Fig. S7, ESI†). Therefore, it is reasonable to assume that this cubic phase is a micellar cubic phase, too,⁴⁸ the same as observed for the homologues with slightly shorter N -terminal chains. However, formation of a micellar cubic phase (Cub_I) at temperatures below a Col_{hex} phase is a bit surprising, as a bicontinuous cubic phase would be expected,^{39,45} but the observed phase sequence could also be explained considering the special core–shell structure of the spheroids. As described above, only a slight increase of the N -terminal chain leads to the bursting of the spheroids with formation of columns. Therefore, thermal expansion of the N -terminal chain has a much stronger effect on mesophase morphology than thermal expansion of the C -terminal chains and this leads to a transition $\text{Cub}_I\text{-Col}_{\text{hex}}$ upon rising temperature. In this way the usually observed phase sequence $\text{Col}_{\text{hex}}\text{-Cub}_I$ on rising temperature,³⁹ which results from a stronger thermal expansion of the aliphatic periphery, is reversed in this case. This means that reducing the temperature has a similar effect as reducing the length of the N -terminal chain.

Columnar phases of the amides A3ⁿ/m. The behavior of the amides **A3ⁿ/m** is different from the previously discussed compounds, as for the amide derivatives **A3ⁿ/m** with $n = 12, 16$ and a short N -terminal chain ($m = 2, 3$) only columnar phase and no Cub_I phases were observed. This indicates that it is more difficult to curve the polar/apolar interfaces of the amide aggregates. In this context it is interesting to note, that for the three-chain amides the number of molecules organized in a slice of the columns with a height of $h = 0.45\text{ nm}$ is a bit smaller

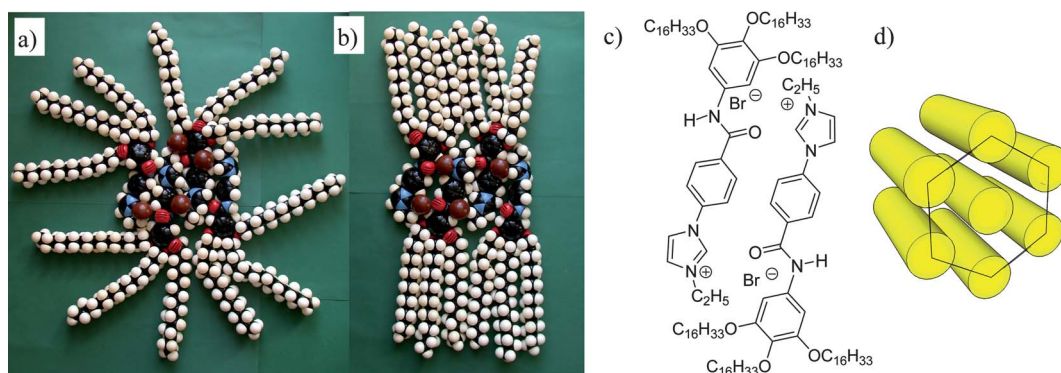


Fig. 13 CPK-models showing the antiparallel organization of four molecules $A3^{16/2}$ in a slice of a column in the Col_{hex} phase: (a) with radial distribution of the alkyl chains, requiring interdigitation of adjacent columns and (b) ribbon-like organization with nearly parallel alkyl chains, in this case time and space averaging of the orientation of the ribbons leads to an on average hexagonal lattice; (c) shows the complete interdigitation of the polar aromatic cores allowing polar interactions between the amide groups and the imidazolium units; (d) shows the arrangement of the column cores on a hexagonal lattice.

($n = 4.5-4.6$) compared to $n = 5.3-6.7$ for the ethers. This could indicate that the benzanilide cores can adopt a more dense packing, probably due to polar interactions between the amide groups and the imidazolium unit of adjacent molecules. This would favor an antiparallel and interdigitated organization of the aromatic cores, as shown in Fig. 13 which reduces the interface curvature between the polar aromatics and the apolar alkyl chains. In addition, the ribbon-like structure of the column cores with a dense antiparallel packing of the rod-like cores makes the aromatic regions more rigid and a further curvature of the polar/apolar interfaces becomes more difficult. Both effects, the reduced interface curvature and the increased aggregate rigidity, remove the Cub_I and Col_{hex} phases of the ether $E3^{16/4}$ and replaces them by a SmA phase in the related amide $A3^{16/4}$. The interdigitated antiparallel organization of the rod-like moieties in the column cores requires fewer molecules to achieve a compact packing in these cores and this leads to the experimentally observed reduction of a_{hex} .

Overall, the amide groups seem to favor intercalation of the aromatic cores and in this way replacing $-CH_2O-$ or $-COO-$ by $-CONH-$ has a similar effect as increasing the length of the N -terminal chains in the ether and ester based imidazolium salts.

Comparison of the compounds shown in Table 10 reveals that, surprisingly, the mesophase stability of the three chain amides $A3^{16/m}$ is considerably reduced in comparison to the related esters $C3^{16/m}$ and ethers $E3^{16/m}$. This is opposite to the trends seen for

the related non-ionic $1H$ -imidazoles and it might also be a result of the antiparallel core packing. In this organization the N -terminal chains can distort the packing of the molecules due to the unfavorable mixing of these short chains with the long C -terminal chains. Also in this respect the effect of exchanging $-CH_2O-/COO-$ linking groups by $-CONH-$ is similar as increasing the length of the N -terminal chain.

3. Conclusions

In summary, two new series of phenylbenzylether ($X = CH_2O$) and benzanilide based ($X = CONH$) rod-like imidazolium salts and their nonionic precursors, the 1-phenyl- $1H$ -imidazoles have been synthesized and the influence of the number and length of the alkyl chain(s) and the structure of the linking group in the aromatic core on their mesophase self-assembly were studied. Upon enlarging the number and length of the C -terminal chains, the sequence $SmA-Col_{hex}-Cub_I/Pm3n$ was found for the ether based and the previously reported ester based imidazolium salts (Scheme 4). In this way they follow the general designing rules for amphiphilic LC molecules where increasing the volume fraction of the aliphatic chains at a given core structure leads to an increasingly negative curvature of the aliphatic-aromatic interface which changes the aggregate morphology from lamellar to spheroidal.³⁹

Table 10 Comparison of the mesophases and transition temperatures of the phenylbenzoate based imidazolium salts $C3^{16/m}$ ³³ with related benzyl-phenylether based imidazolium salts $E3^{16/m}$ and benzanilides $A3^{16/m}$

Compd	X = CH ₂ O ($T^{\circ}C$)	Compd.	X = COO ($T^{\circ}C$)	Compd.	X = CONH ($T^{\circ}C$)
$E3^{16/2}$	Cr 96 Cub_I 217 Iso	$C3^{16/2}$	Cr 98 Cub_I 225 Iso	$A3^{16/2}$	Cr 115 Col_h 189 Iso
$E3^{16/3}$	Cr 89 Cub_I 184 Iso	$C3^{16/3}$	Cr 106 Cub_I 202 Iso	$A3^{16/4}$	Cr 127 (SmA 92) Iso
$E3^{16/4}$	Cr 102 Col_h 145 Iso	$C3^{16/4}$	Cr 109 Col_h 171 Iso		
$E3^{16/5}$	Cr 97 Iso	$C3^{16/5}$	Cr 102 SmA 118 Iso		

For compounds with three *C*-terminal chains, upon only slight enlargement of the *N*-terminal chain the phase sequence $Cub_1-CO_{1hex}-SmA$ is observed, which is opposite to the effect of enlarging the number and length of the *C*-terminal chains. This is due to the core-shell structure of the aggregates where the *N*-alkyl chains fill the core region. In the cores the aromatic-aliphatic interface curvature is positive and hence the effect of increasing the volume of the *N*-terminal chains is opposite to that of the *C*-terminal chains covering the outside of the aggregates with negative curvature. Due to the strong restriction of the space available in the cores of spheroidal and cylindrical aggregates only slight enlargement of the *N*-terminal chains is sufficient to remove these curved aggregates and to replace them by a lamellar structure.

Replacement of the $-COO-$ linkage of the previously described imidazolium salts **C¹Im** by the $-CH_2O-$ group in most cases reduces the melting points and always decreases the mesophase stability, whereas the dependence of the phase type on the number and length of *C*- and *N*-terminal chains is not changed. The reduction of the transition temperature is most probably caused by the enhanced flexibility of the benzylether linkage, distorting the packing of the aromatic cores. Also the reduced polarity, which leads to a reduced incompatibility between the alkyl chains and the aromatic cores, contributes to this effect by reducing the strength of segregation. Nevertheless, due to the lower transition temperatures these ethers are advantageous over the related esters.

The benzanilides incorporating the more polar $-CONH-$ group generally show enhanced melting points and for the non-ionic *1H*-imidazoles also enhanced mesophase stability due to the increased intramolecular polarity contrast between the benzanilide core and alkyl chains. In contrast, the related imidazolium salts with amide groups show lower mesophase stability than the related ethers and esters. The unexpected reduction of mesophase stability by replacing $-CH_2O-/COO-$ by $-CONH-$ suggests that the packing of the amide-based imidazolium salts might be different from the related ether- and ester-based imidazolium salts. It is proposed that the polar intermolecular interaction between the amide moieties and the ionic units of adjacent molecules favor an antiparallel and completely interdigitated packing of the polar rod-like cores, leading to ribbon-like aggregates with reduced aromatic-aliphatic interface curvature, disfavoring the formation of strongly curved interfaces, even if the *N*-terminal chain is very short (Scheme 4). Hence, in this series of compounds it seems to be not possible to achieve the Cub_1 phases with three linear alkyl chains, but branching of the alkyl chain or replacing them by bulkier semiperfluorinated chains^{39e} could enhance the amount of the aliphatic-aromatic interface curvature and in this way could probably lead to spheroidal aggregates.

Overall, these studies provided general clues for the proper design of ionic liquid crystals, especially for tailoring the aggregate structure and the LC temperature range. This contributes to the molecular design of new ILCs for future applications.

Acknowledgements

This work was supported by the National Natural Science Foundation of China (No. 21074105 and No. 20973133), the

Yunnan Science Foundation (2010CD018). MP acknowledges the support by the Cluster of Excellence "Nanostructured Materials" and DFG (FG 1145).

References

- (a) G. Decher, *Science*, 1997, **277**, 1232–1237; (b) C. F. J. Faul and M. Antonietti, *Adv. Mater.*, 2003, **15**, 673–683; (c) C. F. J. Faul, P. Krattiger, B. M. Smarsly and H. Wennemers, *J. Mater. Chem.*, 2008, **18**, 2962–2967; (d) M. Li, R. J. Oakley, H. Bevan, B. M. Smarsly, S. Mann and C. F. J. Faul, *Chem. Mater.*, 2009, **21**, 3270–3274; (e) N. Houbenov, A. Nykanen, H. Iatrou, N. Hadjichristidis, J. Ruokolainen, C. F. J. Faul and O. Ikkala, *Adv. Funct. Mater.*, 2008, **18**, 2041–2047.
- D. R. MacFarlane, J. Huang and M. Forsyth, *Nature*, 1999, **402**, 792–794.
- (a) M. Yoshizawa, W. Xu and C. A. Angell, *J. Am. Chem. Soc.*, 2003, **125**, 15411–15419; (b) A. Noda, M. A. B. H. Susan, K. Kudo, S. Mitsuhashi, K. Hayamizu and M. Watanabe, *J. Phys. Chem. B*, 2003, **107**, 4024–4033; (c) M. A. B. H. Susan, A. Noda, S. Mitsuhashi and M. Watanabe, *Chem. Commun.*, 2003, 938–939.
- (a) S. Ueda, J. Kagimoto, T. Ichikawa, T. Kato and H. Ohno, *Adv. Mater.*, 2011, **23**, 3071–3074; (b) T. Ichikawa, M. Yoshio, A. Hamasaki, J. Kagimoto, H. Ohno and T. Kato, *J. Am. Chem. Soc.*, 2011, **133**, 2163–2169.
- (a) F. Livolant and F. A. Leforestier, *Prog. Polym. Sci.*, 1996, **21**, 1115–1164; (b) G. Zanchetta, *Liq. Cryst. Today*, 2009, **18**, 40–49.
- S. R. Tu, R. Marullo, R. Pynn, R. Bitton, H. Bianco-Peled and M. V. Tirrell, *Soft Matter*, 2010, **6**, 1035–1044.
- D. McLoughlin, M. Emperor-Clerc and D. Langevin, *ChemPhysChem*, 2004, **5**, 1619–1623.
- (a) I. Koltover, T. Salditt, J. O. Radler and C. R. Safinya, *Science*, 1998, **281**, 78–81; (b) C. R. Safinya, K. Ewert, A. Ahmad, H. M. Evans, U. Raviv, D. J. Needleman, A. J. Lin, N. L. Slack, C. G. eorg and C. E. Samuel, *Philos. Trans. R. Soc. London, Ser. A*, 2006, **364**, 2573–2596; (c) A. Bilalov, U. Olsson and B. Lindman, *Soft Matter*, 2011, **7**, 730–742.
- I. J. B. Lin and C. S. Vasam, *J. Organomet. Chem.*, 2005, **690**, 3498–3512.
- K. Binnemans, *Chem. Rev.*, 2005, **105**, 4148–4204.
- J. D. Holbrey and K. R. Seddon, *Clean Prod. Processes*, 1999, **1**, 223; K. R. Seddon, *J. Chem. Technol. Biotechnol.*, 1997, **68**, 351; T. Welton, *Chem. Rev.*, 1999, **99**, 2071; A. Triolo, O. Russina, H.-J. Bleif and E. Di Cola, *J. Phys. Chem. B*, 2007, **111**, 4641–4644; H. Weingaertner, *Angew. Chem., Int. Ed.*, 2008, **47**, 654–670; S. Ahrens, A. Peritz and T. Strassner, *Angew. Chem., Int. Ed.*, 2009, **48**, 7908–7910.
- T. Kato, N. Mizoshita and K. Kishimoto, *Angew. Chem., Int. Ed.*, 2006, **45**, 38–68.
- N. Yamanaka, R. Kawano, W. Kubo, N. Masaki, T. Kitamura, Y. Wada, M. Watanabe and S. Yanagida, *J. Phys. Chem. B*, 2007, **111**, 4763–4769.
- N. Yamanaka, R. Kawano, W. Kubo, T. Kitamura, Y. Wada, M. Watanabe and S. Yanagida, *Chem. Commun.*, 2005, 740–742.
- W. Dobbs, B. Heinrich, C. Bourgeois, B. Donnio, E. Terazzi, M.-E. Bonnet, F. Stock, P. Erbacher, A.-L. Bolcato-Bellemin and L. Douce, *J. Am. Chem. Soc.*, 2009, **131**, 13338–13346.
- M. Yoshio, T. Ichikawa, H. Shimura, T. Kagata, A. Hamasaki, T. Mukai, H. Ohno and T. Kato, *Bull. Chem. Soc. Jpn.*, 2007, **80**, 1836–1841.
- J. H. Olivier, F. Camerel, J. Barbera, P. Retailleau and R. Ziessel, *Chem.–Eur. J.*, 2009, **15**, 8163–8174.
- (a) K. Hoshino, M. Yoshio, T. Mukai, K. Kishimoto, H. Ohno and T. Kato, *J. Polym. Sci., Part A: Polym. Chem.*, 2003, **41**, 3486–3492; (b) M. Yoshio, T. Mukai, H. Ohno and T. Kato, *J. Am. Chem. Soc.*, 2004, **126**, 994–995; (c) M. Yoshio, T. Kagata, K. Hoshino, T. Mukai, H. Ohno and T. Kato, *J. Am. Chem. Soc.*, 2006, **128**, 5570–5577; (d) H. Shimura, M. Yoshio, K. Hoshino, T. Mukai, H. Ohno and T. Kato, *J. Am. Chem. Soc.*, 2008, **130**, 1759–1765; (e) S. Yazaki, Y. Kamikawa, M. Yoshio, A. Hamasaki, T. Mukai, H. Ohno and T. Kato, *Chem. Lett.*, 2008, **37**, 538–539.
- M. R. Imam, M. Peterca, U. Edlund, V. S. K. Balagurusamy and V. Percec, *J. Polym. Sci., Part A: Polym. Chem.*, 2009, **47**, 4165–4193.

- 20 C. O. Osuji, C. Y. Chao, C. K. Ober and E. L. Thomas, *Macromolecules*, 2006, **39**, 3114–3117.
- 21 K. Goossens, P. Nockemann, K. Driesen, K. Driesen, B. Goderis, C. Görrler-Walrand, K. V. Hecke, L. V. Meervelt, E. Pouzet, K. Binnemans and T. Cardinaels, *Chem. Mater.*, 2008, **20**, 157–168.
- 22 (a) Q. X. Zhang, L. S. Jiao, C. S. Shan, P. Hou, B. Chen, X. Y. Xu and L. Niu, *Liq. Cryst.*, 2008, **35**, 765–772; (b) Q. X. Zhang, C. S. Shan, X. D. Wang, L. L. Chen, L. Niu and B. Chen, *Liq. Cryst.*, 2008, **35**, 1299–1305.
- 23 H. Yoshizawa, T. Mihara and N. Koide, *Liq. Cryst.*, 2005, **32**, 143–149.
- 24 J. Fouchet, L. Douce, B. Heinrich, R. Welter and A. Louati, *Beilstein J. Org. Chem.*, 2009, **5**, No. 51.
- 25 P. H. J. Kouwer and T. M. Swager, *J. Am. Chem. Soc.*, 2007, **129**, 14042–14052.
- 26 (a) J. M. Suisse, S. Bellemin-Laponnaz, L. Douce, A. Maise-Francois and R. Welter, *Tetrahedron Lett.*, 2005, **46**, 4303–4305; (b) J. M. Suisse, L. Douce, S. Bellemin-Laponnaz, A. Maise-François, R. Welter, Y. Miyake and Y. Shimizu, *Eur. J. Inorg. Chem.*, 2007, 3899–3905.
- 27 B. El Hamaoui, L. J. Zhi, W. Pisula, U. Kolb, J. Wu and K. Müllen, *Chem. Commun.*, 2007, 2384–2386.
- 28 (a) J. Motoyanagi, T. Fukushima and T. Aida, *Chem. Commun.*, 2004, **1**, 101–103; (b) M. A. Alam, J. Motoyanagi, Y. Yamamoto, T. Fukushima, J. Kim, K. Kato, M. Takata, A. Saeki, S. Seki, S. Tagawa and T. Aida, *J. Am. Chem. Soc.*, 2009, **131**, 17722–17723.
- 29 (a) S. Kumar and K. S. Pal, *Tetrahedron Lett.*, 2005, **46**, 2607–2610; (b) K. S. Pal and S. Kumar, *Tetrahedron Lett.*, 2006, **47**, 8993–8997.
- 30 (a) C. J. Bowles, D. W. Bruce and K. R. Seddon, *Chem. Commun.*, 1996, 1625–1626; (b) C. M. Gordon, J. D. Holbrey, A. R. Kennedy and K. R. Seddon, *J. Mater. Chem.*, 1998, **8**, 2627–2636; (c) J. D. Holbrey and K. R. Seddon, *J. Chem. Soc., Dalton Trans.*, 1999, 2133–2139; (d) G. A. Knight and B. D. Shaw, *J. Chem. Soc.*, 1938, 682–683; (e) E. J. R. Sudhölter, J. B. F. N. Engberts and W. H. De Jeu, *J. Phys. Chem.*, 1982, **86**, 1908–1913.
- 31 X. J. Li, D. W. Bruce and J. M. Shreeve, *J. Mater. Chem.*, 2009, **19**, 8232–8238.
- 32 (a) W. Dobbs, L. Douce and B. Heinrich, *Beilstein J. Org. Chem.*, 2009, **5**, No. 62; (b) J.-H. Olivier, F. Camerel, F. Ulrich, J. Barber and R. Ziessel, *Chem. Eur. J.*, 2010, **16**, 7134–7142; (c) S. Yazaki, M. Funahashi, J. Kagimoto, H. Ohno and T. Kato, *J. Am. Chem. Soc.*, 2010, **132**, 7702–7708; (d) J. E. Baraa, E. S. Hatakeyama, B. R. Wiesenauerb, X. H. Zeng, R. D. Noblea and D. L. Gina, *Liq. Cryst.*, 2010, **37**(12), 1587–1599; (e) F. Xu, K. Matsumoto and R. Hagiwara, *Chem.–Eur. J.*, 2010, **16**, 12970–12976; (f) J. C. Y. Lin, C.-J. Huang, Y.-T. Lee, K.-M. Lee and I. J. B. Lin, *J. Mater. Chem.*, 2011, **21**, 8110–8127; (g) K. Goossens, S. Wellens, K. V. Hecke, L. V. Meervelt, T. Cardinaels and K. Binnemans, *Chem.–Eur. J.*, 2011, **17**, 4291–4306.
- 33 X. H. Cheng, X. Q. Bai, S. Jing, H. Ebert, M. Prehm and C. Tschierske, *Chem.–Eur. J.*, 2010, **16**, 4588–4601.
- 34 (a) P. E. Fanta, *Chem. Rev.*, 1964, **64**, 613–632; (b) T. Yamamoto and Y. Kurata, *Can. J. Chem.*, 1983, **61**, 86–86; (c) J. Lindley, *Tetrahedron Lett.*, 1984, **40**, 1433–1456.
- 35 I. Dierking, *Textures of Liquid Crystals*, Wiley-VCH, Weinheim, 2003.
- 36 The molecular length L was determined in the most extended conformation with all-*trans*-conformation of the alkyl chains using space-filling models (also known CPK models by Corey, Pauling and Koltun), see R. B. Corey and L. Pauling, *Rev. Sci. Instrum.*, 1953, **24**, 621–627.
- 37 This type of interdigitated bilayer structure is assigned as SmA₂ though the d -parameter is significantly smaller than $d = 2L$ and corresponds to $L < d < 2L$, which is usually assigned to double layer smectic phases abbreviated as SmA_d; in SmA_d phases there is an interdigitation of the rod-like aromatic cores leading to the reduction of d to a value smaller than $2L$; however, in the SmA₂ phases reported here, the aromatic parts adopt a non-interdigitated antiparallel end-to-end organization as typical for SmA₂ phases; the reduction of the d -value is in this case due to the interdigitation of the alkyl chains, which retains the end-to-end packing of the rod-like cores and therefore, we assign these phases as SmA₂.
- 38 The shown model is simplified, in reality the alkyl chains are in a molten disordered state and also the aromatic cores are more disordered, a slight interdigitation of the imidazole units is also possible.
- 39 (a) K. Borisch, S. Diele, P. Göring and C. Tschierske, *Chem. Commun.*, 1996, 237–238; (b) K. Borisch, S. Diele, P. Göring, H. Müller and C. Tschierske, *Liq. Cryst.*, 1997, **22**, 427–443; (c) K. Borisch, S. Diele, P. Göring, H. Kresse and C. Tschierske, *Angew. Chem., Int. Ed. Engl.*, 1997, **36**, 2087–2089; (d) K. Borisch, S. Diele, P. Göring, H. Kresse and C. Tschierske, *J. Mater. Chem.*, 1998, **8**, 529–543; (e) X. H. Cheng, K. Das, S. Diele and C. Tschierske, *Langmuir*, 2002, **18**, 6521–6529.
- 40 (a) T. Noguchia, K. Kishikawab and S. Kohmotob, *Liq. Cryst.*, 2008, **35**, 1043–1050; (b) X. L. Zhou, T. Narayanan and Q. Li, *Liq. Cryst.*, 2007, **34**, 1243–1248; (c) B.-K. Cho, A. Jain, S. M. Gruner and U. Wiesner, *Science*, 2004, **305**, 1598–1601; (d) T. Kato, T. Matsuoka, M. Nishii, Y. Kamikawa, K. Kanie, T. Nishimura, E. Yashima and S. Ujiie, *Angew. Chem., Int. Ed.*, 2004, **43**, 1969–1972; (e) A. Kohlmeier, D. Janietz and S. Diele, *Chem. Mater.*, 2006, **18**, 1483–1489; (f) M. Lehmann and M. Jahr, *Chem. Mater.*, 2008, **20**, 5453–5456; (g) S. Coco, C. Cordovilla, B. Donnio, P. Espinet, M. J. Garcia-Casas and D. Guillon, *Chem.–Eur. J.*, 2008, **14**, 3544–3552.
- 41 X. H. Cheng, S. Diele and C. Tschierske, *Angew. Chem., Int. Ed.*, 2000, **39**, 592–595.
- 42 B. M. Rosen, C. J. Wilson, D. A. Wilson, M. Peterca, M. R. Imam and V. Percec, *Chem. Rev.*, 2009, **109**, 6275–6540.
- 43 (a) S. D. Hudson, H.-T. Jung, V. Percec, W.-D. Cho, G. Johansson, G. Ungar and V. S. K. Balagurusamy, *Science*, 1997, **278**, 449–452; (b) V. Percec, W.-D. Cho, P. E. Mosier, G. Ungar and D. J. P. Yearley, *J. Am. Chem. Soc.*, 1998, **120**, 11061–11070; (c) V. Percec, M. N. Holerca, S. Uchida, W.-D. Cho, G. Ungar, Y.-S. Lee and D. J. P. Yearley, *Chem.–Eur. J.*, 2002, **8**, 1106–1117; (d) D. J. P. Yearley, G. Ungar, V. Percec, M. N. Holerca and G. Johansson, *J. Am. Chem. Soc.*, 2000, **122**, 1684–1689.
- 44 H. J. Deutecher, R. Frach, C. Tschierske, H. Zaszke, in *Selected Topics in Liquid Crystal Research*, Ed. H.-D. Koswig, Akademie Verlag Berlin, 1990, pp.1–18.
- 45 (a) S. T. Hyde, in *Handbook of Applied Surface and Colloid Chemistry*, Ed. K. Holmberg, Wiley, 2001, pp 299–232; (b) S. Diele, *Curr. Opin. Colloid Interface Sci.*, 2002, **7**, 333–342; (c) M. Imperor-Clerc, *Curr. Opin. Colloid Interface Sci.*, 2005, **9**, 370–376.
- 46 G. Ungar and X. Zeng, *Soft Matter*, 2005, **1**, 95–106.
- 47 (a) K. Fontell, K. K. Fox and E. Hansson, *Mol. Cryst. Liq. Cryst. Lett. Sect.*, 1985, **1**, 9–17; (b) K. Fontell, *Colloid Polym. Sci.*, 1990, **268**, 264–285; (c) P. Zihler and R. D. Kamien, *J. Phys. Chem. B*, 2001, **105**, 10147–10158; (d) G. M. Grason, B. A. DiDonna and R. D. Kamien, *Phys. Rev. Lett.*, 2003, **91**, 058304; (e) J. Charvolin and J. F. Sadoc, *J. Phys.*, 1988, **49**, 521–526; (f) R. Vargas, P. Mariani, A. Gulik and V. Luzzati, *J. Mol. Biol.*, 1992, **225**, 137–145.
- 48 No bicontinuous cubic phase with $Pm3n$ lattice is known,⁴⁵ therefore a bicontinuous structure, as expected if the phase sequence is considered, is unlikely. Also the lattice parameter of this cubic phase is in the same range as observed for E3¹⁶/3 (see Table 7); the slight increase of a_{cub} by 0.4 nm with respect to E3¹⁶/3 is in line with the increase of m from 3 to 4.